# Modeling and Control Design of Hybrid – LCC and VSC based – HVDC Systems

Christoph Hahn, *Member, IEEE,* Andreas Geuß, Matthias Luther, *Member, IEEE*
Friedrich-Alexander-University of Erlangen-Nuremberg (FAU)
Institute of Electrical Energy Systems
Erlangen, Germany
christoph.hahn@fau.de, andreas.geuss@fau.de, matthias.luther@fau.de

***Abstract*—This paper reveals an approach for dynamic modeling and control design of hybrid High-Voltage Direct Current (HVDC) systems. In this case a hybrid system is supposed to be a connection of different converter topologies as Line Commutated (LCC) and Voltage Source Converters (VSC). Modeling will be based on the mathematical correlations of the respective topologies and therefore a model for each converter type is carried out. These models can be merged regarding the fact of balanced energy terms.**

**A control strategy for the hybrid HVDC system is presented, where the LCC Converter controls the voltage of the DC link and the VSC Converter is in *P*/*Q* control mode and hence is responsible for DC current regulation. Due to the comparison of the generic stability model with an EMT (Electro-Magnetic Transient) HVDC model the consistence of the dynamic behavior is shown and a comprehensive large signal model of a hybrid HVDC system which can be used for power system stability studies is revealed.**

***Index Terms*—Dynamic Modeling, Hybrid HVDC Systems, Line Commutated Converter (LCC), Voltage Source Converter (VSC), HVDC Control Strategies.**

## I. Introduction

After Fukushima nuclear disaster the German government decided a transition of the national energy policy and therefore the use of HVDC systems has gained a lot of interest as it is stated in the German Grid Development plan [1]. One of the main topics is the handling of the large amount of upcoming offshore wind parks in the North and East Sea and their integration into the onshore AC grid. Due to the use of submarine cables AC transmission is only suitable up to a distance of around 80 km [2]. Once this distance is exceeded the use of HVDC systems is the preferred technology.

But not only in Germany the energy transition is a current issue since the US government under President Obama just recently has moved towards a Clean Power Plan [3]. Therefore the use of technology in order to integrate renewable energy sources into the grid will arise also in the USA.

LCC HVDC technology is already well known since decades and the most important technical background can be found in standard literature as [4], [5] and [6]. The Modular Multilevel Converter for HVDC applications was introduced from Lesnicar and Marquardt in 2003 [7] but has been investigated intensively in the last years.

As depicted in Figure 1 a hybrid HVDC system could be used especially for the integration of large offshore windfarms into onshore AC grids [8].

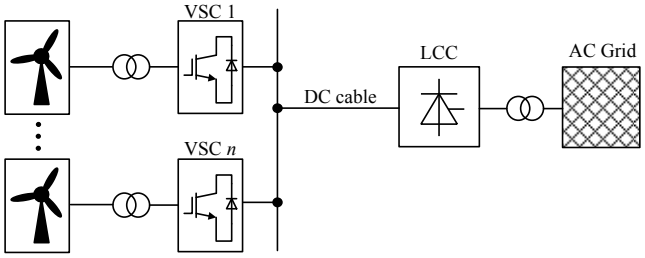


Figure 1: Topology of an integration concept of an offshore windfarm via a hybrid HVDC system

Using a hybrid HVDC system for this integration concept the advantages of both technologies can be merged and the disadvantages compensated:

- Less space requirements for VSC converters on offshore stations since no filters are necessary
- Black start capability of VSC for offshore AC grids
- Independent *P*/*Q* control of VSC for offshore grids
- Higher power rating for a single onshore LCC conv.
- Minimization of losses due to the use of LCC technology
- Less installation costs for LCC technology

Modeling approaches for LCC HVDC systems have already been carried out in [9] and also MMC VSC HVDC systems are well described e.g. in [10]. The hybrid system has not been intensively studied so far and also detailed control concepts for such a system are still missing although some first approaches can be found in [8] and [11].

Due to the numerous advantages this concept could be a preferable solution for the integration of large scale offshore windfarms in future and therefore a detailed novel modeling and control design approach will be presented in this paper

978-1-5090-2157-4/16/$31.00 ©2016 IEEE

which could be used for power system stability studies. The developed dynamic mathematical model will be verified by a comparison with an EMT model where also energy, horizontal and vertical balancing controllers are included. Simulations will show the energization and startup process of the entire system with the involved controllers.

## II. Modeling of Hybrid HVDC Systems

As already mentioned modeling approaches for LCC and VSC HVDC systems have been carried out in [9] and [10] respectively and these approaches might also be used in a form adapted for hybrid systems. In the first section the LCC converter modelling is described followed by the VSC converter and DC circuit modeling. The models are then connected via the terms of energy balance.

### A. LCC Converter Modeling

The basic structure of a twelve pulse LCC converter is depicted in Figure 2 where $V_p$ and $V_s$ are the RMS (Root Mean square) AC voltages of the primary and secondary side of the converter. $X_c$ is the converter transformer reactance and $I_{DC}$ and $V_{DC}$ are the direct current and voltage respectively.

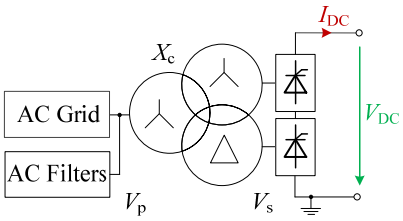


Figure 2: Basic structure of a twelve pulse LCC Converter

Based on the equivalent circuit of Figure 2 the derivation of the DC voltage in dependence on the AC side quantities and the firing angle $\alpha$ might be obtained from [4]:

$$V_{DC} = B\frac{3\sqrt{2}}{\pi}V_s\cos\alpha - B\frac{3}{\pi}X_c I_{DC}. \tag{1}$$

The parameter $B$ is one ($B=1$) for six-pulse HVDC systems and $B$ equals two ($B=2$) for twelve-pulse units. Changes of the firing angle due the control system will not apply immediately to the direct voltage due to an average firing delay of $60°/B$ which can be modeled as a dead time element and linearized to a delay first order element through Taylor series expansion [12] where $f$ is the AC grid frequency:

$$F_d(s) = e^{-sT_d} \approx \frac{1}{1+sT_d}, \text{ where } T_d = \frac{1}{6B}\frac{1}{f}. \tag{2}$$

As the LCC converter is proposed for inverter operation in the outlined system the extinction angle is of high importance for the later explained control structure in order to avoid commutation failures. The extinction angle can be determined once the overlap $u$ is known:

$$\gamma = 180° - \alpha - u. \tag{3}$$

The overlap or commutation angle $u$ can be derived by applying Kirschhoff's law to the equivalent circuit of the LCC converter during the state of commutation which yields in a differential equation where the solution for $u$ is shown in (4).

$$u = \arccos\left(\cos(\alpha) - \frac{2\omega I_{DC} L_c}{\sqrt{2}V_s}\right) - \alpha. \tag{4}$$

Consequently the active and reactive power consumption of the LCC converter can be stated:

$$P = V_{DC} I_{DC}, \tag{5}$$

$$Q = P\tan\left[\arccos\left(\frac{\cos\alpha + \cos(\alpha+u)}{2}\right)\right]. \tag{6}$$

A block diagram of the mathematical model of the LCC converter using the derived equations can then be developed and is shown in Figure 3.

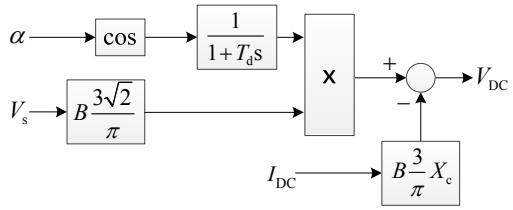


Figure 3: Block diagram of the mathematical model of the LCC converter

The firing angle $\alpha$ and the AC voltage $V_s$ serve as input value for the dynamic model as well as the direct current $I_{DC}$. Depending on the configuration of the DC circuit – as shown later on – the topology could also be changed and hence $V_{DC}$ serves as an input and $I_{DC}$ as an output value.

### B. VSC MMC Converter Modeling

The VSC MMC converter in contrast to classical two or three level pulse width modulation (PWM) based VSC converters bases on a series connection of several submodules in each converter arm which exist in half- or full-bridge configuration [10]. Due to the large amount of submodules the sinusoidal grid voltage can be adapted very accurately and harmonic distortion is limited to a minimum [13]. Therefore the first modeling approach is the replacement of the series connection of submodules with controlled voltage sources. Mathematical analysis can then be based on the single phase equivalent circuit diagram which is depicted in Figure 4.

In steady state operation the grid current $i_N$ is shared equally among the positive and negative converter arm at the point of common coupling and therefore the positive and negative arm current can be defined as:

$$i_p = \frac{1}{2}i_N + i_{diff}, \tag{7}$$

$$i_n = -\frac{1}{2}i_N + i_{diff}. \tag{8}$$

978-1-5090-2157-4/16/$31.00 ©2016 IEEE

Equations (7) and (8) can be transformed in order to reveal a mathematical description for the grid current $i_N$ and the circulating current $i_{diff}$:

$$i_N = i_p - i_n, \tag{9}$$

$$i_{diff} = \frac{1}{2}\left(i_p + i_n\right). \tag{10}$$

Regarding Figure 4 three mesh equations comprising the grid voltage $v_N$ and the upper converter arm voltage $v_{Cp}$, the lower converter arm voltage $v_{Cn}$ and the voltage at point of common coupling $v_{PCC}$ can be revealed.

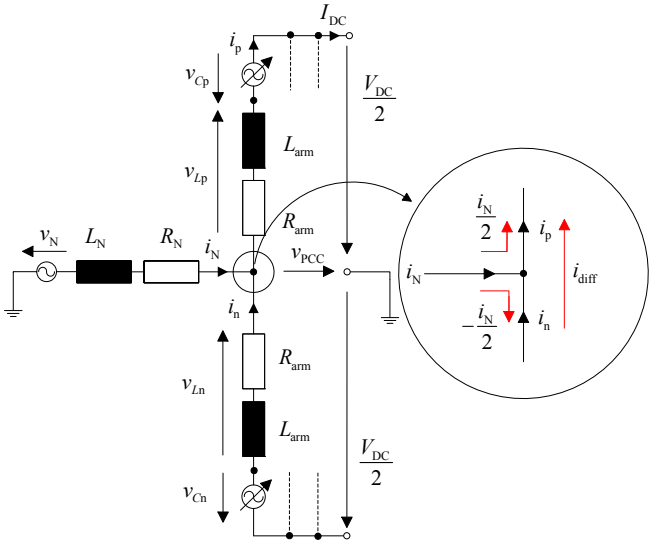


Figure 4: Single phase equivalent circuit diagram of MMC VSC converter with controlled voltage sources

Subtracting the mesh equations containing $v_{Cp}$ and $v_{Cn}$ and applying the definition of equation (10) the appropriate differential equation for $i_{diff}$ can be stated [10]:

$$\frac{\mathrm{d}i_{diff}}{\mathrm{d}t} + \frac{R_{arm}}{L_{arm}} i_{diff} = \frac{1}{2L_{arm}}\left(\left(v_{Cn} + v_{Cp}\right) - V_{DC}\right). \tag{11}$$

With the definition of the grid current according to equation (9) the appropriate differential equation for $i_N$ can be determined:

$$\left(L_N + \frac{L_{arm}}{2}\right)\frac{\mathrm{d}i_N}{\mathrm{d}t} + \left(R_N + \frac{R_{arm}}{2}\right) i_N = v_N - \underbrace{\frac{v_{Cn} - v_{Cp}}{2}}_{e_{PCC}}. \tag{12}$$

Comparing equation (11) and (12) reveals, that $i_{diff}$ can be controlled by the sum of $v_{Cp}$ and $v_{Cn}$; $i_N$ can be controlled by the respective difference. Since the sum and the difference of two quantities are linearly independent $i_{diff}$ and $i_N$ can be controlled independently.

In order to obtain a mathematical model in the Laplace domain where control design can be based on the park transformation is applied to the three phase system of equation (12). After a few calculations the differential equation system reveals in the dq frame under neglection of the zero system component due to the assumption of a symmetrical system where $R = R_N + R_{arm}/2$ and $L = L_N + L_{arm}/2$:

$$\begin{pmatrix} v_{N\_d} \\ v_{N\_q} \end{pmatrix} - \begin{pmatrix} e_{PCC\_d} \\ e_{PCC\_q} \end{pmatrix} = \begin{pmatrix} L & 0 \\ 0 & L \end{pmatrix} \frac{\mathrm{d}}{\mathrm{d}t} \begin{pmatrix} i_{N\_d} \\ i_{N\_q} \end{pmatrix} + \begin{pmatrix} R & -\omega L \\ \omega L & R \end{pmatrix} \begin{pmatrix} i_{N\_d} \\ i_{N\_q} \end{pmatrix}. \tag{13}$$

This system of equations can be transformed to the Laplace domain and solved for the currents $i_{N\_d}$ and $i_{N\_q}$ which are acting as output variables of the system. The block diagram representing the MMC VSC converter model can then be presented in Figure 5.

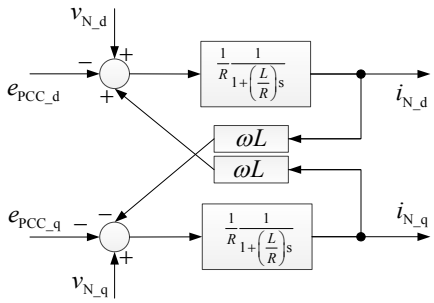


Figure 5: Block diagram of the AC side model of the MMC VSC converter

## C. DC Circuit Modeling

Considering a DC cable connecting the LCC and VSC converter a T-line equivalent circuit could be used for its representation as shown in Figure 6.

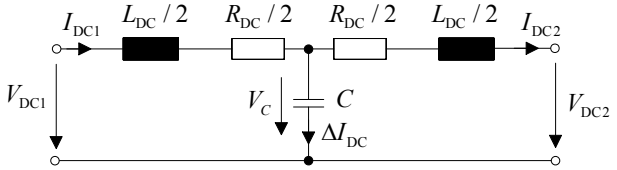


Figure 6: DC line equivalent circuit considering the distributed submodule capacities

Considering the dynamic behavior of the distributed submodules in each converter arm, the DC line capacity can be extended with an equivalent capacitor comprising the dynamic behavior of the distributed submodule capacities in the three converter arms of the VSC:

$$C = C_{cable} + \frac{C_{SM}}{n_{SM}} \cdot 3. \tag{14}$$

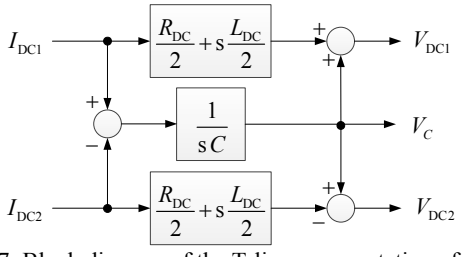


Figure 7: Block diagram of the T-line representation of the DC circuit

Determining the differential equations of the proposed T-line model and transferring the set of equations into the Laplace domain reveals in a block diagram as depicted in Figure 7.

### D. Concatenation of the Converter and DC Circuit Models

The models derived in the previous sections can now be combined via the terms of energy balance. As the outlined voltage sources of the MMC VSC are a connection of capacitors in reality they only have a limited energy storage capability. Therefore, the power which is obtained from the VSC connected AC grid has to be transferred to the LCC connected AC grid via the DC circuit. This fact can be used in order to combine the models via their respective power equations:

$$P = \frac{3}{2} v_{\mathrm{N\_d}}\, i_{\mathrm{N\_d}} = V_{\mathrm{DC}} I_{\mathrm{DC}}. \tag{15}$$

As the modeling of the hybrid HVDC system has been described in this section the control structure is described in the next chapter.

## III. Control of Hybrid HVDC Systems

Control strategies for LCC and VSC systems are well known and have been outlined e.g. in [9] and [10]. However, these control strategies can be used but have to be adapted for hybrid HVDC systems.

### A. LCC Converter Control in a hybrid HVDC system

In the proposed system shown in Figure 1 the LCC converter operates in inverter mode since the power is transferred from the wind park to the onshore AC grid. As it will be described in the next section the VSC converter is capable of independent active and reactive power control and therefore the LCC converter is suggested to work in DC voltage control mode. Nevertheless, it is of high importance to add an extinction angle controller to the LCC converter since it operates in inverter mode and therefore the firing angle is close to 180° degree and hence commutation failures are very likely to occur.

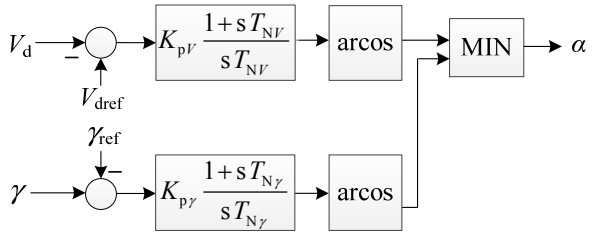


Figure 8: Proposed control structure for LCC converter

In a classical configuration the inverter side LCC converter also comprises a marginal current controller since it might happen that the rectifier reaches its upper firing angle limitation due to an AC voltage drop and therefore cannot control the DC current anymore. As the DC side of the MMC VSC converter can be controlled independently of the AC side as determined in the previous chapter this controlling function is not required.

### B. VSC Converter Control

As MMC VSC converters are capable of independent active and reactive power control it is of advantage to keep its control structure unchanged in order to guarantee the highest flexibility.

The converter model was developed in the dq frame and therefore the controller will be in the dq frame too. A cascaded control system with an inner current controller and an outer power controller will be applied to the system as depicted in Figure 9.

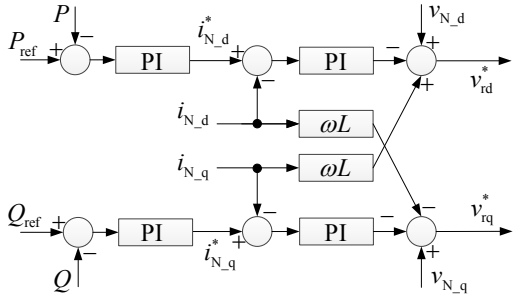


Figure 9: Proposed control structure of the MMC VSC converter

In order to eliminate the coupling terms of the d and q quantities in the model (see Figure 5) a decoupling filter is applied to the controller as illustrated in the middle of Figure 9. As the LCC converter is responsible for the voltage control in the DC link the MMC VSC converter therefore guarantees the right DC current via the active power control.

The entire block diagram of the hybrid HVDC system with its appropriate control system is illustrated in Figure 10. $T_{\mathrm{a}}$ might represent the time lag due to the discretization of the control signals.

## IV. Results and Comparison with an EMT Modell

The developed model and its appropriate control structure were implemented in the numerical computing environment MATLAB/Simulink® and the parameters according to Table I were applied and can be obtained from [9], [10] and [14]. A verification of the developed math. stab. model (Index MSM) with an EMT model which was built up in MATLAB/ Simulink® using the SimPowerSystems® toolbox was performed. The series connection of submodules was replaced with controlled voltage sources and energy, horizontal and vertical balancing controllers were applied in the EMT model.

Table I: parameter set of the proposed system

| | | | |
|---|---|---|---|
| $f_{\mathrm{N1}} = f_{\mathrm{N2}}$ | 50 Hz | $P_{\mathrm{ref}}$ | 1000 MW |
| $V_{\mathrm{N1}}$ | 333 kV | $V_{\mathrm{DCref}}$ | 640 kV |
| $V_{\mathrm{N2}}$ | 300 kV | $\gamma_{\mathrm{ref}}$ | 25° |
| $R_{\mathrm{N1}} = R_{\mathrm{N2}}$ | 0.425 Ω | $K_{\mathrm{p\_}i}$ | 0.5 |
| $L_{\mathrm{N1}} = L_{\mathrm{N2}}$ | 85.5 mH | $T_{\mathrm{N\_}i}$ | 0.1 sec |
| $R_{\mathrm{arm}}$ | 0.47 Ω | $K_{\mathrm{p\_}P\_Q}$ | 0.5 |
| $L_{\mathrm{arm}}$ | 50 mH | $T_{\mathrm{N\_}P\_Q}$ | 0.2 sec |
| $R_{\mathrm{DC}}$ | 5 Ω | $K_{\mathrm{p}V}$ | 0.5 |
| $L_{\mathrm{DC}}$ | 85 mH | $T_{\mathrm{N}V}$ | 0.03 sec |
| $C_{\mathrm{SM}}$ | 4.5 mF | $K_{\mathrm{p}\gamma}$ | 0.3 |
| $n_{\mathrm{SM}}$ | 400 | $T_{\mathrm{N}\gamma}$ | 0.05 sec |

978-1-5090-2157-4/16/$31.00 ©2016 IEEE

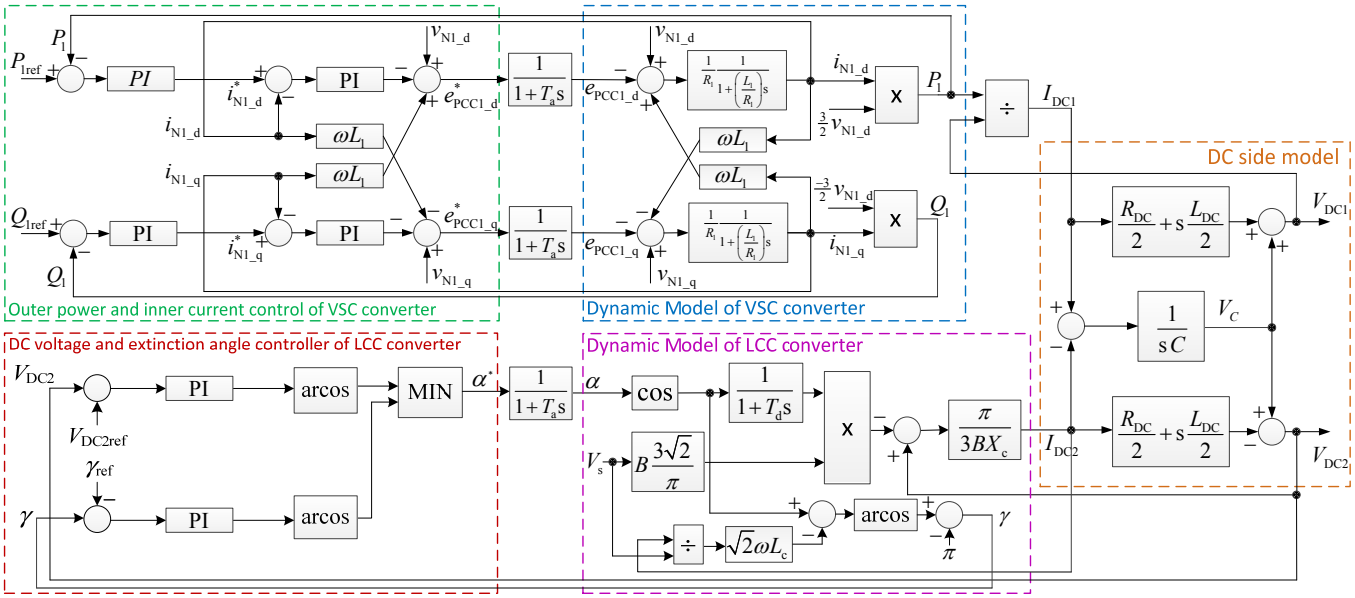


Figure 10: Block diagram of the entire mathematical stability model and its appropriate control structure of the hybrid HVDC system

In order to show the functioning of the developed model and its proposed control structure a startup process of the hybrid HVDC system is performed.

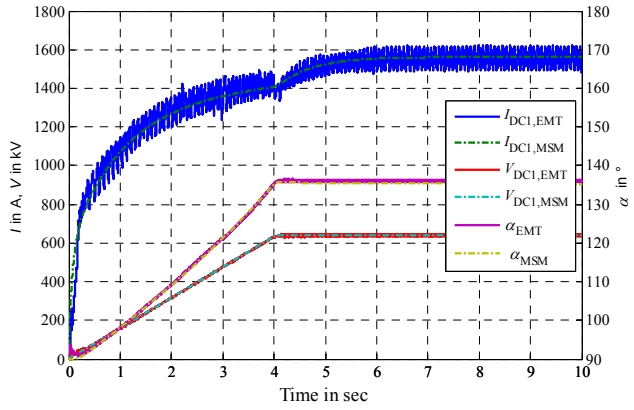


Figure 11: DC Voltage, DC current and firing angle during the startup process of the hybrid HVDC system

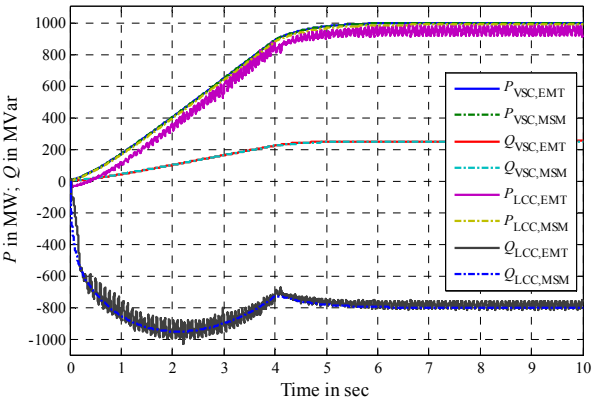


Figure 12: Active and reactive power at LCC and VSC converter during the startup process of the hybrid HVDC system

Figure 11 shows the DC voltage, DC current and firing angle during the startup process. The reference value of the DC voltage at the LCC converter is ramped up from $t = 0$ sec to $t = 4$ sec as well as the active and reactive power set point at the VSC converter as shown in Figure 12. The firing angle starts at 90° and as the LCC converter is in inverter mode increases up to its stationary value. The extinction angle is always lower as its reference value and the appropriate controller doesn't intervene during the startup process. Since the DC voltage and the active power is ramped up as described the DC current reveals via the previously described power balance. It can be seen that the DC current rises very fast and reaches its nominal value once the active power reaches the desired reference value.

The DC side capacity smooths the DC voltage well and therefore the DC current in the EMT model has ripples due to the switching characteristic of the twelve pulse LCC converter. Once the DC capacity is downsized the ripples in DC current will decrease but therefore DC voltage ripples will arise. This optimization problem can also be diminished due to the use of specific harmonic filters which are not applied in this model.

Figure 12 illustrates the LCC and VSC AC side active and reactive power. As the VSC converter is in rectifier operation its active power is slightly higher due to losses in the system. The ripples of the DC current can also be seen in the active power of the LCC converter of the EMT model since no filters are applied. The active power of the VSC converter in contrast is very smooth since the ripples of the DC side are not transferred to the AC side due to their independence as indicated in earlier.

The reactive power of the VSC converter can be controlled independently of the active power and is therefore set to 250 MVar. The reactive power consumption of the LCC converter is dependent on the active power, the firing angle

and the overlap according to equation (6). During the startup process the firing angle is close to 90° and hence the reactive power consumption of the LCC converter is very high. Once the firing angle is rising the reactive power consumption decreases. Nevertheless, the stationary reactive power is still very high since the stationary firing angle is around 125°. A firing angle around 150° at the inverter is desirable as it still keeps enough distance in order to prevent commutation failures.

Overall the comparison of both models shows very good matching results and therefore the mathematical model could be validated. Furthermore the proposed control scheme works as desired and is capable of performing a startup process of the hybrid HVDC system.

## V. Conclusion

This paper shows a novel approach of modelling and control design for a hybrid HVDC system. As indicated a hybrid HVDC solution could gain a lot of interest in the future for the connection of large scale offshore wind parks to the onshore AC grid and therefore it is crucial to develop a model with its appropriate control structure which can be used for power system stability studies.

The mathematical stability model of the LCC and VSC converter as well as the DC circuit was developed based on the transfer functions in the Laplace domain and subsequently the models were merged via the terms of energy balance.

A control structure for the hybrid HVDC system was presented where the LCC converter is capable of controlling the DC link voltage and the VSC converter still has the highest flexibility of controlling active and reactive power independently.

A comparison of the developed model with an EMT model was shown and both models demonstrate a high level of consistency. Therefore the developed model can be used for power system stability studies as it comprises a detailed large signal model with its entire control scheme.

## References


[1] 50Hz, Amprion, TenneT, TransnetBW – TSO's of Germany, "Grid development plan – 2nd draft" (Netzwentwicklungsplan Strom - 2. Entwurf), Berlin, Germany, 2014.

[2] B. M. Buchholz, D. Povh and D. Retzmann, "Stability Analysis for large Power System Interconnections in Europe," in *Proc. IEEE Power Tech*, St. Petersburg, Russia, June 2005.

[3] United States Environmental Protection Agency – EPA, "Federal Plan Requirements for Greenhouse Gas Emissions from Electric Utility Generating Units Constructed on or Before January 8, 2014", Federal Register, EPA-HQ-OAR-2015-0199, August 2015.

[4] E. W. Kimbark, *Direct Current Transmission*. John Wiley & Sons: New York, London, Sydney, Toronto, 1971.

[5] J. Arrillaga, *High Voltage Direct Current Transmission*. The Institution of Electrical Engineers: London, UK, 2008.

[6] K. R. Padiyar, *HVDC Power Transmission Systems*. New Academic Science Limited: Kent, UK, 2011.

[7] A. Lesnicar and R. Marquardt, "An innovative modular multilevel converter topology suitable for a wide power range," in *2003 IEEE Bologna Power Tech*, Bologna, Italy, June 2003.

[8] R. E. Torres-Olguin, M. Molinas and T. Undeland, "Hybrid HVDC connection of large offshore wind farms to the AC grid," in *Proc. IEEE International Symposium on Industrial Electronics (ISIE)*, Hangzhou, China, May 2012.

[9] C. Hahn, A. Semerow, M. Luther, and O. Ruhle, "Generic Modeling of a Line Commutated HVDC System for Power System Stability Studies," in *2014 IEEE PES Transmission & Distribution Conference and Exposition*, Chicago, USA, April 2014.

[10] C. Hahn, M. Burkhardt, A. Semerow, M. Luther and O. Ruhle, "Generic modeling of a self-commutated multilevel VSC HVDC system for power system stability studies," in *Proc. Applied Power Electronics Conference and Exposition (APEC)*, pp. 2672-2677, Charlotte, USA, March 2015.

[11] W. Pan, Y. Chang and H. Chen, "Hybrid Multi-terminal HVDC System for Large Scale Wind Power," in *Proc. IEEE Power System Conference and Exposition*, Atlanta, USA, Oct. 2006.

[12] C. Hahn, A. Müller and M. Luther, "A novel approach to select HVDC - controller parameters by using a decoupling filter," in *Proc. International Conference on Renewable Energies and Power Quality (ICREPQ'13)*, Bilbao, Spain, March 2013.

[13] J. Dorn, H. Huang, and D. Retzmann, "Novel Voltage-Sourced Converters for HVDC and FACTS Applications," in *Proc. CIGRE Conference*, Osaka, Japan, Oct. 2007.

[14] S. Dennetière, H. Nguefeu, H. Saad and J. Mahseredjian, "Modeling of modular multilevel converters for the France-Spain link," in *Proc. Int. Conf. Power System Transients*, Vancouver, Canada, July 2013.


## Biographies

**Christoph Hahn** (M'2012) received his Dipl.-Ing. degree from the University of Erlangen-Nuremberg, Germany, in 2011. Currently he is research associate and working towards a Ph.D. at the Institute of Electrical Energy Systems at the University of Erlangen-Nuremberg, Germany. His research interests lie in the field of HVDC modeling and control.

**Andreas Geuß** received his B.Sc. and M.Sc. degree from the University of Erlangen-Nuremberg, Germany, in 2013 and 2015 respectively. Currently he is working as commissioning engineer for HVDC systems at Siemens AG in Erlangen, Germany.

**Matthias Luther** (M'2011) studied electrical engineering and received his Ph.D. at the Technical University of Brunswig, Germany in 1992. From 1993 he held different functions and management positions in the electricity industry at PreussenElektra, E.ON Netz and TenneT TSO. Since 2011 he is professor and holds the Chair of Electrical Energy Systems at the University of Erlangen-Nuremberg, Germany.

978-1-5090-2157-4/16/$31.00 ©2016 IEEE